Proceedings of the 21st ICSMGE, Vienna, Austria, 14 – 19 June 2026. Pistrol, Adam & Schweiger (eds.)
Published by: ÖGG, Austrian Society for Geomechanics, Salzburg, Austria, ISBN 978-3-9503898-4-5
https://doi.org/10.53243/ICSMGE2026-1672

Elastic solutions for a head-restrained pile subjected to a passive load

Ivo Bellezza, Marta di Sante, Evelina Fratalocchi, Francesco Mazzieri
Department S.I.M.A.U, Università Politecnica delle Marche, Ancona, Italy, i.bellezza@staff.univpm.itt

ABSTRACT: The paper analyses a single head-restrained flexible passive pile embedded in a soil profile consisting of an unstable layer overlying a stable one. The pile segment in the unstable layer is subjected to a linear distribution of the load whereas the pile response is evaluated by assuming a uniform modulus of subgrade reaction in the stable layer. Closed-form expressions are derived for the pile deflection and bending moment at the pile head. Analytical solutions for infinitely flexible and rigid piles have been obtained as special cases of the general solution. A novel rational flexibility criterion for passive piles is also proposed. A numerical example is finally presented to illustrate the application of the derived solution.

KEYWORDS: landslides, slope stabilization, soil-structure interactions.

1 INTRODUCTION

Vertical piles are subjected to a passive load when they are installed in a moving soil. If the soil movement is vertical the well-known phenomenon of the negative skin friction occurs which implies a supplementary axial force and pile downdrag. On the other hand, lateral soil movement induces shear forces and bending moments that the piles must be able to resist without serviceability or ultimate limit state failure. Typical examples of piles subjected to lateral movement are piles adjacent to deep excavations (Leung et al. 2000; Goh et al. 2003), or piles supporting bridge abutment close to approach embankments (Poulos 1996) or piles used to stabilize landslides.

In this latter context a variety of design and analysis methods have been developed to calculate the factor of safety of pile-reinforced slopes (Ito et al., 1979, 1981, 1982; Chow, 1996; Hassiotis et al., 1997; Cai and Ugai, 2000, 2011; Ausilio et al., 2001; Jeong et al., 2003; Won et al., 2005; Wei and Cheng, 2009; Ellis et al., 2010; Yamin and Liang 2010; Kourkoulis et al. 2011, 2012; Ashour and Ardalan, 2012; Di Laora and Fioravante 2018; Lei et al., 2022). Finite element methods generally allow simultaneously to capture pile and slope behavior, but they require a specific expertise in soil and pile modelling, selection of the input parameters and the use of three-dimensional computer codes with extensive computational resources. In practice an uncoupled analysis is generally performed in which the pile response and slope stability are considered separately.

Piles installed in unstable slopes are designed with the purpose to stop the soil movement and the success of this technique depends on the capacity to develop the arc effect. Some studies suggest a center to center spacing of three/four pile diameter as the most cost-effective solution (Poulos, 1995; Kourkoulis et al., 2011; Ellis et al., 2010). The length of a pile in the unstable layer is generally known and the main design issues include the selection of the embedded length and the prediction of the internal forces and deflections of the piles.

In the literature two main methods are available to analyze piles embedded in a soil subject to lateral movement: the *displacement-based* and the *pressure-based* methods.

The displacement-based method (Chen and Poulos, 1997) allows realistic loading conditions, but only if an accurate assessment of lateral soil movement can be made, it is generally possible to obtain a satisfactory prediction of the pile response,

In the pressure-based method the aforesaid drawback is overcome assuming that the pile segment in the moving soil is subjected to an assigned load, in the same direction of the soil movement. For a conservative design, the passive load can be assumed equal to the ultimate soil pressure (Ito et al., 1979, 1981). This assumption is strictly valid if the piles are sufficiently embedded in the stable layer to develop the failure mechanism named mode C or "flow mode" in previous studies (e.g. Viggiani, 1981; Poulos, 1995; Di Laora et al., 2017; Bellezza and Caferri, 2018) and that the soil movement is sufficient to fully mobilize the pile-soil ultimate pressure (Bellezza, 2024).

To predict the pile displacement and maximum bending moment it is necessary to model the soil-pile interaction below the sliding surface and the use of a specific computer program.

For simplified soil profiles closed-form expressions are available for a ready evaluation of the pile response but most analytical solutions refer only to infinitely flexible or rigid piles (Ito et al., 1981; Guo, 2014; Bellezza, 2020). Recently, Bellezza and Fratalocchi (2025) derived a general analytical solution for free-head piles of whichever flexural stiffness subjected to a linear passive load using the subgrade reaction method. Considering that actual slope-stabilizing piles are often connected by a beam, in this paper the analysis is extended to piles with unrotated head with the purpose of obtaining analytical expressions for the pile deflections and maximum bending moment, to be used in preliminary design phase. It will be shown that the case of flexible and rigid piles can be viewed as special cases of the general solution. A novel rational criterion to establish whenever a passive pile with unrotated head can be assumed flexible is finally proposed.

2 METHOD OF ANALYSIS

2.1 *Basic assumptions*

A pile of total length L with a constant flexural stiffness EJ is considered. A portion of the pile of length L_1 lies in the unstable layer, whereas the remaining portion of length L_2 (= λL_1) is embedded in a stable layer.

An upward (z_1) and a downward (z_2) abscissa with origin at the sliding surface are taken for the pile segment in the unstable and stable zone, respectively (Fig.1a). Similarly to previous studies on stabilizing piles (e.g. Cai and Ugai, 2003, 2011; Lei et al., 2022), the soil reaction in the stable layer is assumed to be fully elastic with a uniform modulus of subgrade reaction, E_S. This assumption is reasonably valid in overconsolidated clays (Viggiani et al., 2012).

In the unstable layer a linear distribution of the passive load is considered with a value q_0 and q_1 at the sliding surface and at the ground surface, respectively, with a resultant force S_0 applied at a distance μL_1 above the sliding surface (Fig.1a). The assumed linear distribution agrees with distributions proposed in the literature for the ultimate soil reaction (Ito and Matsui, 1975; De Beer and Carpentier, 1977; Broms, 1964; Fleming et al., 2009). The values of q_0 and q_1 depend on several factors, including soil type and pile spacing (Poulos, 1995; Georgiadis et al., 2013).

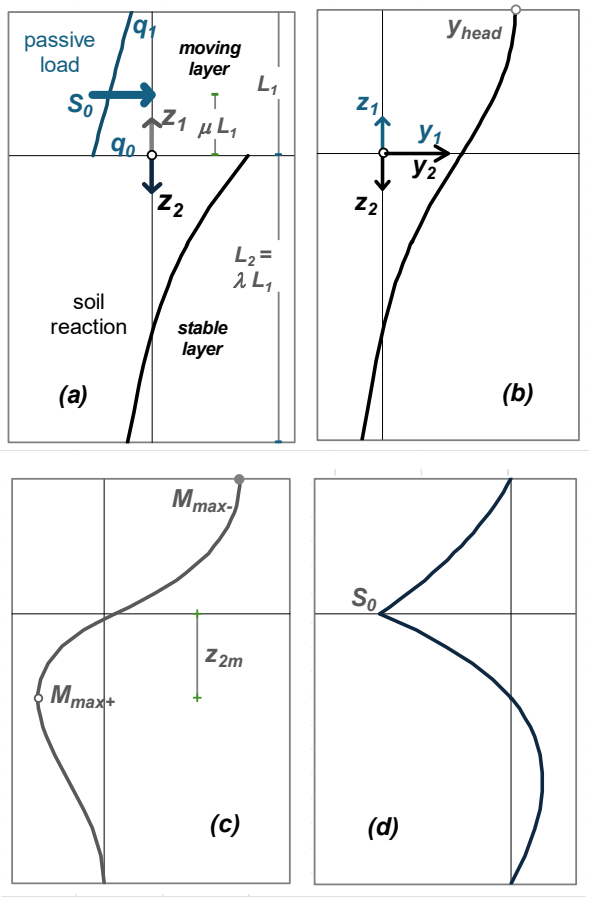

Figure 1. Typical response of a single passive pile with unrotated head: (a) load per unit length; (b) pile deflection; (c) bending moment; (d) shear force.

2.2 *Governing equations*

The deflections of the pile in the unstable and stable zone (Fig.1b) are governed by:

$$EJ\frac{d^4y_1}{dz_1^4} = q_0 - m_1 z_1 \qquad 0 \le z_1 \le L_1 \tag{1a}$$

$$EJ\frac{d^4y_2}{dz_2^4} + E_S y_2 = 0 \qquad 0 \le z_2 \le L_2 \tag{1b}$$

where $m_1 = (q_0 - q_1)/L_1$.

The general solutions of (1) are:

$$y_1(z_1) = -\frac{m_1}{120EJ}z_1^5 + \frac{q_0}{24EJ}z_1^4 + k_4 z_1^3 + k_3 z_1^2 + k_2 z_1 + k_1 \tag{2a}$$

$$y_2(z_2) = \exp(-\beta z_2)\,(A_1\cos\beta z_2 + A_2\sin\beta z_2) + \exp(\beta z_2)\,(A_3\cos\beta z_2 + A_4\sin\beta z_2) \tag{2b}$$

where k_i and A_i are constants and $\beta = (E_s/(4EJ))^{0.25}$.

The slopes, bending moments and shear forces in the two pile segments can be obtained as:

$$\theta_1(z_1) = -\frac{m_1}{24EJ}z_1^4 + \frac{q_0}{6EJ}z_1^3 + 3k_4 z_1^2 + 2k_3 z_1 + k_2 \tag{3a}$$

$$\theta_2(z_2) = \beta\exp(-\beta z_2)[-A_1(\cos\beta z_2 + \sin\beta z_2) + A_2(\cos\beta z_2 - \sin\beta z_2)] + \beta\exp(\beta z_2)\,[A_3(\cos\beta z_2 - \sin\beta z_2) + A_4(\cos\beta z_2 + \sin\beta z_2)] \tag{3b}$$

$$M_1(z_1) = EJ\left(-\frac{m_1}{6EJ}z_1^3 + \frac{q_0}{2EJ}z_1^2 + 6k_4 z_1 + 2k_3\right) \tag{4a}$$

$$M_2(z_2) = 2EJ\beta^2\{\exp(-\beta z_2)\,[A_1\sin\beta z_2 - A_2\cos\beta z_2] + \exp(\beta z_2)\,[-A_3\sin\beta z_2 + A_4\cos\beta z_2]\} \tag{4b}$$

$$S_1(z_1) = EJ\left(-\frac{m_1}{2EJ}z_1^2 + \frac{q_0}{EJ}z_1 + 6k_4\right) \tag{5a}$$

$$S_2(z_2) = 2EJ\beta^3\{\exp(-\beta z_2)[A_1(\cos\beta z_2 - \sin\beta z_2) + A_2(\cos\beta z_2 + \sin\beta z_2)] - \exp(\beta z_2)\,[A_3(\cos\beta z_2 + \sin\beta z_2) - A_4(\cos\beta z_2 - \sin\beta z_2)]\} \tag{5b}$$

The values of the constants k_i and A_i are calculated by imposing: (1) the continuity conditions of the deflection, slope, bending moment and shear force at the depth of the sliding surface ($z_1 = z_2 = 0$); (2) the boundary conditions at the pile head ($z_1 = L_1$) and (3) the boundary conditions at the pile tip ($z_2 = L_2$):

$$y_1\big|_{z_1=0} = y_2\big|_{z_2=0} \Longrightarrow k_1 = A_1 + A_3 \tag{6a}$$

$$\theta_1\big|_{z_1=0} = -\theta_2\big|_{z_2=0} \Longrightarrow k_2 = \beta(A_1 - A_2 - A_3 - A_4) \tag{6b}$$

$$M_1\big|_{z_1=0} = M_2\big|_{z_2=0} \Longrightarrow k_3 = -\beta^2(A_2 - A_4) \tag{6c}$$

$$S_1\big|_{z_1=0} = -S_2\big|_{z_2=0} \Longrightarrow 3k_4 = -\beta^3(A_1 + A_2 - A_3 + A_4) \tag{6d}$$

$$\theta_1\big|_{z_1=L_1} = 0 \Longrightarrow -\frac{m_1}{24EJ}L_1^4 + \frac{q_0}{6EJ}L_1^3 + 3k_4 L_1^2 + 2k_3 L_1 = 0 \tag{7a}$$

$$S_1\big|_{z_1=L_1} = 0 \Longrightarrow -\frac{m_1}{2EJ}L_1^2 + \frac{q_0}{2EJ}L_1 + 6k_4 = 0 \tag{7b}$$

$$M_2\big|_{z_2=L_2} = 0 \Longrightarrow \exp(-\psi_2)\,[A_1\sin\psi_2 - A_2\cos\psi_2] - \exp(\psi_2)\,[A_3\sin\psi_2 - A_4\cos\psi_2] = 0 \tag{8a}$$

$$S_2\big|_{z_2=L_2} = 0 \Longrightarrow \exp(-\psi_2)\,[A_1(\cos\psi_2 - \sin\psi_2) + A_2(\cos\psi_2 + \sin\psi_2)] - \exp(\psi_2)\,[A_3(\cos\psi_2 + \sin\psi_2) - A_4(\cos\psi_2 - \sin\psi_2)] = 0 \tag{8b}$$

where $\psi_2 = \beta L_2$.

2.3 *Dimensionless solutions*

The Equations (6)-(8) form a linear system with 8 unknowns (k_i and A_i). After some algebraic manipulations the solutions can be conveniently expressed in dimensionless form as:

$$k_{1n} = k_1\left(\frac{E_S L_1}{S_0}\right) = 2C_1\psi_1 + 4C_2\psi_1^2 + 2C_3(\mu + 1/6)\psi_1^3 \tag{9a}$$

$$k_{2n} = k_2\left(\frac{E_S L_1^2}{S_0}\right) = 4C_3\psi_1^3 + 4C_4(\mu + 1/6)\psi_1^4 \tag{9b}$$

$$k_{3n} = k_3\left(\frac{E_S L_1^3}{S_0}\right) = -2C_3\psi_1^3 + 2C_5(\mu + 1/6)\psi_1^5 \tag{9c}$$

$$k_{4n} = k_4\left(\frac{E_S L_1^4}{S_0}\right) = -2\psi_1^4/3 \tag{9d}$$

$$A_{1n} = A_1\left(\frac{E_S L_1}{S_0}\right) = (C_1 + C_4)\psi_1 + (2C_2 + C_3 + C_5)\psi_1^2 + (C_3 + C_4)(\mu + 1/6)\psi_1^3 \tag{10a}$$

$$A_{2n} = A_2\left(\frac{E_S L_1}{S_0}\right) = (C_3 + C_4)\psi_1 - (C_3 - C_5)\psi_1^2 - (C_4 + C_5)(\mu + 1/6)\psi_1^3 \tag{10b}$$

$$A_{3n} = A_3\left(\frac{E_s L_1}{S_0}\right) = (C_1 - C_4)\psi_1 + (2C_2 - C_3 - C_5)\psi_1^2 + (C_3 - C_4)(\mu + 1/6)\psi_1^3 \quad (10c)$$

$$A_{4n} = A_4\left(\frac{E_s L_1}{S_0}\right) = (C_4 - C_3)\psi_1 + (C_5 - C_3)\psi_1^2 + (C_5 - C_4)(\mu + 1/6)\psi_1^3 \quad (10d)$$

where $\psi_1 = \beta L_1$ and C_1, C_2, C_3, C_4 and C_5 are auxiliary functions of $\psi_1$and ψ_2 (Figure 2) defined as:

$$C_1 = \frac{\cosh^2\psi_2 + \cos^2\psi_2}{2\psi_1(\sinh^2\psi_2 - \sin^2\psi_2) + \sinh 2\psi_2 + \sin 2\psi_2} \quad (11a)$$

$$C_2 = \frac{\sinh\psi_2 \cosh\psi_2 - \sin\psi_2 \cos\psi_2}{2\psi_1(\sinh^2\psi_2 - \sin^2\psi_2) + \sinh 2\psi_2 + \sin 2\psi_2} \quad (11b)$$

$$C_3 = \frac{\cosh^2\psi_2 - \cos^2\psi_2}{2\psi_1(\sinh^2\psi_2 - \sin^2\psi_2) + \sinh 2\psi_2 + \sin 2\psi_2} \quad (11c)$$

$$C_4 = \frac{\sinh\psi_2 \cosh\psi_2 + \sin\psi_2 \cos\psi_2}{2\psi_1(\sinh^2\psi_2 - \sin^2\psi_2) + \sinh 2\psi_2 + \sin 2\psi_2} \quad (11d)$$

$$C_5 = \frac{\sinh^2\psi_2 - \sin^2\psi_2}{2\psi_1(\sinh^2\psi_2 - \sin^2\psi_2) + \sinh 2\psi_2 + \sin 2\psi_2} \quad (11e)$$

The expressions (9)-(10) explicitly contain the stabilizing force S_0 provided by the pile. According to the current design procedures (e.g. Poulos, 1995) this force is estimated before the pile response is calculated.

Once the values of k_i and A_i are known, the pile deflections, slopes, bending moments and shear forces at any depth can be obtained by (2), (3), (4) and (5), respectively.

2.4 *Pile head deflection*

The pile head deflection is obtained by (2a) for $z_1 = L_1$:

$$y_{head} = y_1\big|_{z_1=L_1} = -\frac{m_1}{120EJ}L_1^5 + \frac{q_0}{24EJ}L_1^4 + k_4 L_1^3 + k_3 L_1^2 + k_2 L_1 + k_1 \quad (12)$$

Substituting into (12) the values of the constants k_i given by (9), the normalized pile head deflection can be expressed by:

$$y_{head}\frac{E_s L_1}{S_0} = 2C_1\psi_1 + 4C_2\psi_1^2 + 2C_3(\mu + 7/6)\psi_1^3 + [4C_4(\mu + 1/6) - (3\mu + 1)/5]\psi_1^4 + 2C_5(\mu + 1/6)\psi_1^5 \quad (13)$$

2.5 *Maximum bending moment*

For an unrotated-head pile the negative bending moment (M_{max-}) at the pile head (Figure 1c) can be calculated by (4a) for $z_1 = L_1$:

$$M_{max-} = M_1\big|_{z_1=L_1} = EJ\left(-\frac{m_1}{6EJ}L_1^3 + \frac{q_0}{2EJ}L_1^2 + 6k_4 L_1 + 2k_3\right) \quad (14)$$

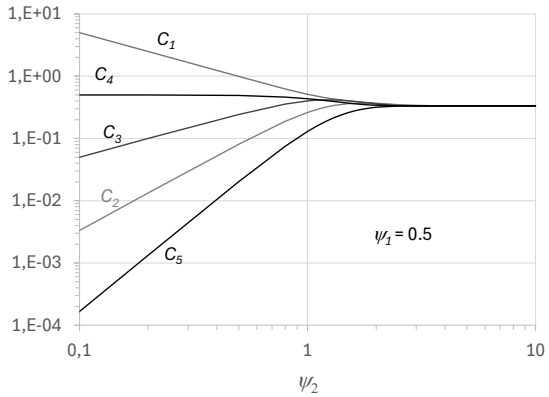

Figure 2. Example of trends of the auxiliary functions C_i versus ψ_2 for $\psi_1 = 0.5$.

Substituting (11c) and (11d) into (14), and rearranging the terms yield:

$$\frac{|M_{max-}|}{S_0 L_1} = \mu + C_3/\psi_1 - C_5(\mu + 1/6)\psi_1 \quad (15)$$

In some cases a positive maximum bending moment (M_{max+}) can develop in the pile segment embedded in the stable layer (Figure 1c). The depth of M_{max+} (z_{2m}) is obtained by imposing null the shear force in (5b) and by *numerically* solving the following transcendent equation:

$$\tan\psi_m = \frac{\exp(2\psi_m)(A_{4n} - A_{3n}) + A_{1n} + A_{2n}}{\exp(2\psi_m)(A_{4n} + A_{3n}) + A_{1n} - A_{2n}} \quad (16)$$

where $\psi_m = \beta z_{2m}$.

Then, M_{max+} is calculated by:

$$\frac{M_{max+}}{S_0 L_1} = \frac{\cos\psi_m}{2\psi_1^2 \exp\psi_m}\left\{\begin{matrix} A_{1n}\tan\psi_m - A_{2n} \\ -\exp(2\psi_m)(A_{3n}\tan\psi_m - A_{4n})\end{matrix}\right\} \quad (17)$$

Table 1 lists the calculated values of M_{max+} for selected combinations of ψ_1, λ and μ.

2.6 *Infinitely flexible piles*

As shown in Figure 2, for increasing ψ_2 all the auxiliary functions C_i tend to the same value $0.5/(1 + \psi_1)$. Therefore, simplified expressions can be written for k_i and A_i (Table 2).

The pile deflection and the maximum negative bending moment given by (13) and (15) become:

$$y_{head,F}\frac{E_s L_1}{S_0} = \psi_1 + \psi_1^2 + \left(\mu + \frac{1}{6}\right)\psi_1^3 + \left(\frac{2}{5}\mu - \frac{1}{30}\right)\psi_1^4 \quad (18)$$

$$\frac{|M_{max-.F}|}{S_0 L_1} = \frac{1 + 2\mu\psi_1 + (\mu - 1/6)\psi_1^2}{2\psi_1(1 + \psi_1)} \quad (19)$$

Also for the maximum positive bending moment in the stable layer a closed-form expression can be obtained:

$$\frac{M_{max+,F}}{S_0 L_1} = \left(2\psi_1 \sin\psi_{m,F} \exp\psi_{m,F}\right)^{-1} \quad (20)$$

where $\psi_{m,F}$ is given by:

$$\psi_{m,F} = \tan^{-1}\frac{1 + \psi_1}{\psi_1 + (\mu + 1/6)\psi_1^2} \quad (21)$$

Table 1. Normalized positive maximum bending moments for some combinations of λ, ψ_1 and μ.

λ	ψ_1	μ = 1/3	μ = 1/2	μ = 2/3
1	2	0.1874	0.2303	0.2751
	3	0.2164	0.2696	0.3248
	4	0.2188	0.2787	0.3404
1.5	1.5	0.1998	0.2352	0.2724
	2	0,2176	0,2599	0,3045
	2.5	0.2168	0.2651	0.3156
2	1	0.1700	0.1949	0.2209
	1.5	0.2233	0.2578	0.2942
	2	0.2187	0.2608	0.3052
2.5	1	0.2220	0.2472	0.2736
	1.5	0.2255	0.2596	0.2956
3	1	0.2418	0.2662	0.2917
	1.5	0.2256	0.2597	0.2958

Table 2. Values of the constant k_i and A_i for the case of infinitely flexible pile segment in the stable layer.

Constants $k_{in,F}$	Constants $A_{in,F}$
$k_{1n,F} = \frac{\psi_1+2\psi_1^2+(\mu+1/6)\psi_1^3}{1+\psi_1}$	$A_{1n,F} = \frac{\psi_1+2\psi_1^2+(\mu+1/6)\psi_1^3}{1+\psi_1}$
$k_{2n,F} = \frac{2\psi_1^3+2(\mu+1/6)\psi_1^4}{1+\psi_1}$	$A_{2n,F} = \frac{\psi_1-(\mu+1/6)\psi_1^3}{1+\psi_1}$
$k_{3n,F} = \frac{(\mu+1/6)\psi_1^5-\psi_1^3}{1+\psi_1}$	$A_{3n,F} = 0$
$k_{4n,F} = -2\psi_1^4/3$	$A_{4n,F} = 0$

Eqs. (18)-(21) reproduce the solution of Ito et al. (1981) in a simpler, compacted and dimensionless form.

2.7 *Infinitely rigid piles*

For increasing flexural stiffness, EJ, the pile tends to move horizontally with a null rotation along the whole pile.

For $\beta \to 0$ (i.e. $\psi_1 \to 0$; $\psi_2 \to 0$), the auxiliary functions C_i can be approximated by the McLaurin series as:

$$C_1 \cong \frac{1}{2\psi_2};\ C_2 \cong \frac{\psi_2^2}{3};\ C_3 \cong \frac{\psi_2}{3};\ C_4 \cong \frac{1}{2};\ C_5 \cong \frac{\psi_2^3}{6} \qquad (22)$$

Then, substituting (22) into (13) and neglecting higher infinitesimals, the expression for the normalized pile head deflection simplifies in:

$$y_{head,R}\frac{E_S L_1}{S_0} \cong \frac{\psi_1}{\psi_2} = \frac{1}{\lambda} \qquad (23)$$

The maximum bending moment is always at the pile head, and it can be calculated as:

$$\frac{|M_{max,R}|}{S_0 L_1} = \mu + \frac{1}{2}\lambda \qquad (24)$$

3 RESULTS AND DISCUSSION

3.1 *Effect of ψ_1 and λ on the pile head deflection*

Figure 3 shows the normalized pile head deflection $y_{head,n}$ (= $y_{head}\ E_S L_1/S_0$) as a function of ψ_1 for different values of λ. For an assigned value of λ all curves follow a similar trend and two zones can be distinguished. For low values of ψ_1, $y_{head,n}$ remains practically constant and equal to the value of the rigid pile given by Equation (23); then $y_{head,n}$ starts to increase at increasing ψ_1. As expected, the pile head deflection is always inversely proportional to the embedment ratio λ. As an example, for $\psi_1 = 1$, $y_{head,n}$ is about 3.38 and 2.61 for λ =1 and $\lambda = 3$, respectively. The effect of λ on $y_{head,n}$ is maximum for rigid piles ($\psi_1 = 0$) and it tends to vanish at increasing ψ_1 when all curves converge to the curve relevant to an infinitely flexible pile (dashed line in Figure 3), analytically defined by Equation (18).

3.2 *Effect of ψ_1 and λ on the maximum bending moment*

Figure 4 shows both the normalized negative maximum bending moment ($M_{max\text{-}n}$ developed at the pile head) and the positive maximum bending moment (M_{max+n} developed along the pile shaft) at varying ψ_1 for different values of λ.

For a given value of λ, the trend of the curves of $M_{max\text{-}n}$ versus ψ_1 is similar to that of Figure 3. For low values of ψ_1 $M_{max\text{-}n}$ remains practically unchanged at varying ψ_1 with the value of a rigid pile (equation 24); then it starts to decrease (in absolute value) at increasing ψ_1, with a rate of decrease dependent on λ.

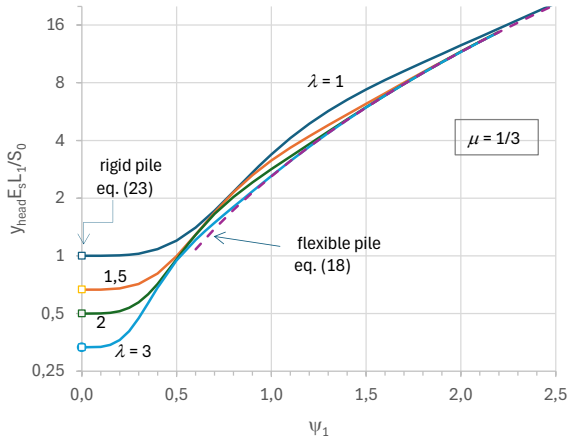

Figure 3. Effect of the dimensionless length ψ_1 and of the embedment ratio λ on the normalized pile head deflection for $\mu = 1/3$.

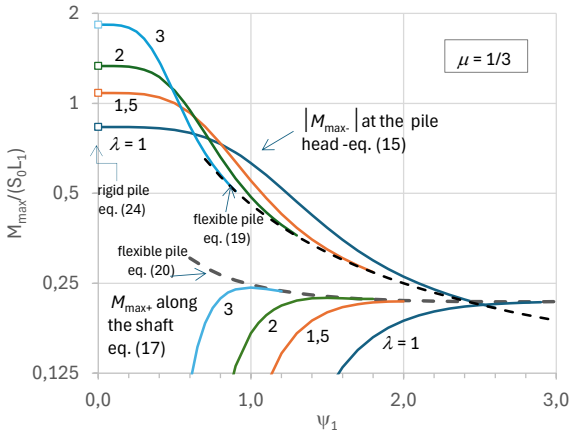

Figure 4. Normalized maximum bending moment vs the dimensionless length ψ_1 for different values of λ with $\mu = 1/3$.

It is worth noting that the positive maximum bending moment starts to develop when ψ_1 exceeds a minimum value that decreases at increasing λ. More importantly, for values of ψ_1 exceeding a threshold value ψ_1* the maximum bending moment on the pile develops no longer at the head but along the shaft. As shown in Figure 4, for μ = 1/3 and λ > 1.5 this threshold value ψ_1* is about 2.42, obtained by equalizing Equations (19) and (20). However, the threshold value ψ_1* depends on the distribution of the passive load (i.e. μ); as an example, for $\mu = 2/3$ the threshold value increases to about 4.48. In the range $1/3 < \mu < 2/3$, ψ_1* can be accurately calculated by a linear interpolation between the above values as $0.36 + 6.18\ \mu$.

The crossover of the curves in Figure 4 indicates that the trend of M_{max} versus λ depends on the value of ψ_1. In Figure 5 the normalized maximum bending moment at the pile head is plotted versus λ for different values of ψ_1 at which the bending moment at the pile head (in absolute value) is always greater than the maximum positive bending moment along the pile shaft (i.e. $M_{max} = |M_{max\text{-}}|$). As expected, for some values of ψ_1 M_{max} peaks for a given value of λ (λ_p). The values of λ_p are found to decrease at increasing ψ_1, whereas λ_p is less sensitive to variation of μ; as an example, for $\psi_1 = 0.5$, $\lambda_p = 2.334$ and $\lambda_p = 2.253$ for $\mu = 1/3$ and $\mu = 2/3$, respectively. Only for relatively high values of ψ_1 M_{max} monotonically decreases at increasing λ, as λ_p is outside the range of practical interest (i.e. $\lambda_p < 1$). Finally, it can be observed that the effect of λ on M_{max} disappears at increasing λ as all curves tend to reach the maximum bending moment of the flexible piles (eq. 19) which depend no longer on λ but only on ψ_1 and μ.

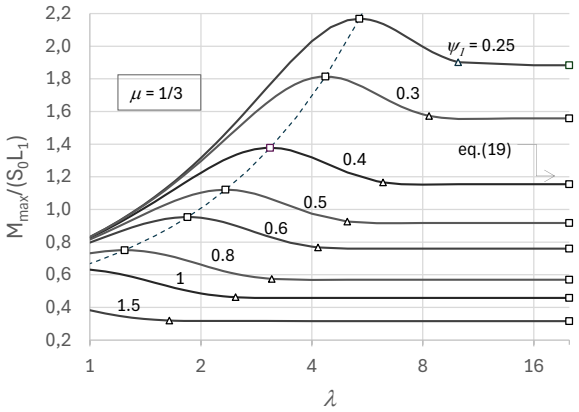

Figure 5. Normalized maximum bending moment vs the embedment ratio λ for different values of ψ_1 with $\mu = 1/3$.

3.3 *Effect of μ on pile head deflection and maximum bending moment*

Equation (13) clearly indicates that the normalized pile head deflection $y_{head,n}$ increases linearly with μ, all other factors being equal. Only for rigid piles (eq.23) $y_{head,n}$ is independent of μ. Also the negative maximum moment given by Equation (15) is a linear function of μ with a gradient equal to (1- $C_5\psi_1$). On the contrary, the form of eq. (17) implies that the correlation between the positive maximum bending moment and μ is not strictly linear, but the errors involved assuming a linear correlation are negligible. In fact, it is easy to check that the values of M_{max+} in Table 1 for $\mu = 0.5$ practically coincide with the average of the values of M_{max+} for $\mu = 1/3$ and $\mu = 2/3$.

3.4 *Flexibility criterion*

Figure 5 indicates that in some ranges of ψ_1 and λ the values of M_{max} calculated by the rigorous solution practically coincide with those obtained for flexible piles by Equation (19). To quantify the range of applicability of the expressions of flexible piles to real piles, a relative difference of 1% is initially considered (triangular symbols in Figure 5). A similar approach can be applied to check the range of validity of Equation (18) for the pile head deflection.

Figure 6 shows some pairs of values of ψ_1 and λ for which $M_{max} = 1.01M_{max,F}$ and $y_{head} = 1.01y_{head,F}$ for the extreme values of μ. As shown in Figure 6 the points can be conveniently interpolated by a power law correlation: $\psi_1 = a\ \lambda^b$ where a and b are fitting parameters.

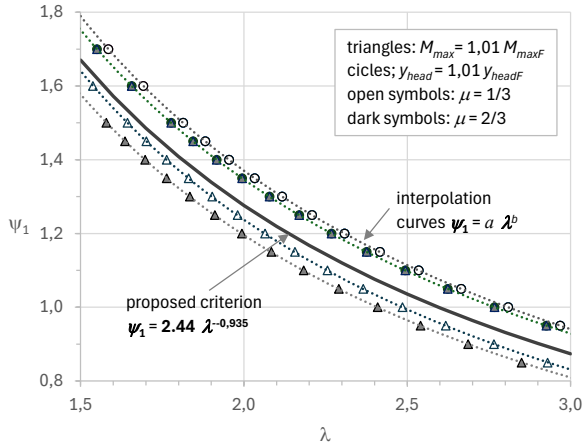

Figure 6. Pairs of values of λ and ψ_1 which meet the flexibility criteria.

It is evident that, the relative percentage error being equal, the criterion based on the head deflection is more conservative than that based on M_{max}, whereas the distribution of the passive load (i.e. μ) has a minor influence. For sake of simplicity a unique average criterion of flexibility for passive piles with unrotated head is here proposed based on 2% relative error on y_{head} for $\mu = 1/3$:

$$\psi_1 \lambda^{0.935} \geq 2.44 \qquad (25)$$

If this condition is hold, in the investigated range of λ the relative errors on M_{max} using (19) are less than 1%.

4 NUMERICAL EXAMPLE

Consider a slope made of 3 m of unstable silty sand (unit weight γ = 18 kN/m^3, friction angle ϕ = 30°) underlaid by a stable overconsolidated clay (E_s = 36 MPa). To stabilize the slope a row of bored piles with unrotated head is used (D = 1 m, L = 10 m; EJ =2'000 MNm^2). The maximum stabilizing force is obtained assuming that the piles in the moving layer are subjected to the soil ultimate pressure. For a pile spacing of 4D it is reasonably to consider the ultimate soil pressure of an isolated pile; therefore, according to Fleming et al. (2009), a maximum shear force S_0 = 729 kN/pile is derived for $\mu = 1/3$ and $m_1 = D\gamma K_P^2$=162 kN/m^2 (where K_P = 3 is the Rankine passive earth pressure coefficient).

For the assigned input, the dimensionless length ψ_1 (= βL_1) and the embedment ratio $\lambda = L_2/L_1$ are calculated as 0.777 and 2.333, respectively (i.e. ψ_2 = 1.813). Then, the normalized pile head deflection is obtained by (13) as 1.859 (i.e. y_{head} = 1.859 S_0/E_sL_1 = 0.0125 m). For $\psi_1 < \psi_1^*$ (= 2.445), the maximum bending moment develops at the pile head, and it is calculated by (15) as M_{max}/S_0L_1 = 0.6455, which implies M_{max} = 1'412 kNm. For sake of completeness the maximum positive bending moment along the pile shaft is numerically computed by (16) and (17) as about 281 kNm at a depth $z_{2m} \cong$ 3.16 m.

The calculated values of y_{head} and M_{max} can be considered as the upper bounds of the actual values if the required stabilizing force is less than 729 kN/pile. In such a case, the pile behavior should be evaluated by numerical methods, which analyze the pile response before the development of the soil ultimate state (e.g., Bellezza et al., 2017; Lei et at. 2023; Bellezza, 2024).

5 SUMMARY AND CONCLUSIONS

An analytical method based on the subgrade reaction approach was presented to analyze a single pile with an unrotated head subjected to a passive load. A uniform modulus of subgrade reaction is assumed in the stable layer whereas a generic linear load is considered on the pile segment in the moving layer. Closed-form equations are derived for the pile head deflection and bending moment at the pile head for pile with a finite flexural stiffness. Tabulated values are provided to evaluate the maximum bending moment along the shaft. For infinitely flexible and rigid piles simplified solutions are also derived, which agree with previous studies. A novel flexibility criterion for passive piles is also proposed.

The results of a parametric study can be summarized as follows:

- as expected, the normalized pile head deflection decreases at increasing the pile embedment λ and at decreasing the dimensionless length ψ_1;
- as far as the maximum bending moment is concerned, the results indicate that for pile of high flexibility M_{max} can develop also on the pile shaft and not necessarily at the

pile head. Moreover, for a given value of ψ_1, the increase of the embedment ratio does not imply necessarily a reduction of M_{max} and the use of the solution for flexible piles can be unconservative.

If the passive load is based on the ultimate soil pressure, the present solution gives conservative estimates for both y_{head} and M_{max} and it can be particularly useful in pre-dimensioning phase for a quick evaluation of the response of single passive piles. On the other hand, the proposed solution becomes unconservative in the presence of soil plasticization and it is limited to the condition of a fully elastic soil response in the stable layer.

The accuracy of the proposed solutions decreases in soil profiles where the hypothesis of a uniform modulus of subgrade is not reasonable, and an average modulus of subgrade reaction must be necessarily assumed. However, the solutions derived in this paper are rigorous from a mathematical point of view and they can be effectively used as a benchmark to validate more sophisticated numerical analyses.

6 REFERENCES

Ashour, M. and Ardalan, H. 2012. Analysis of pile stabilized slopes based on soil–pile interaction. *Computers and Geotechnics* 39, 85–97.

Ausilio, E., Conte, E, and Dente, G. 2001 Stability analysis of slopes reinforced with piles. *Computers and Geotechnics* 28(8), 591–611.

Bellezza, I. 2020. Closed-form expressions for a rigid passive pile in a two-layer soil. *Géotechnique Letters* 10(2), 242-249.

Bellezza, I. 2024. Elastic–Plastic Analysis of Rigid Passive Piles in Two-Layered Soils. *Geotech Geol Eng* 42:2299–2320.

Bellezza, I. and Caferri, L. 2018. Ultimate lateral resistance of passive piles in non-cohesive soils. *Géotechnique Letters* 8(1), 5-12.

Bellezza, I. and Fratalocchi, E. 2025. Analytical solutions for pile subjected to a passive load. *Géotechnique Letters* 15, https://doi.org/10.1680/jgele.24.00148.

Bellezza, I., Caferri, L., Di Sante, M., Fratalocchi, E. and Mazzieri, F. 2017. Elastic-plastic analysis of passive rigid piles in cohesionless soils. *Proc. XIX ICSMGE,* Seoul, South Korea, 2723-2726.

Broms, B. 1964. Lateral resistance of piles in coehesionless soils. *J. Soil Mech. Found. Div. ASCE* 90, 123-156.

Cai, F. and Ugai, K. 2000. Numerical analysis of the stability of a slope reinforced with piles. *Soils and Foundations* 40(1), 73–84.

Cai, F. and Ugai, K. 2003. Response of flexible piles under laterally linear movement of the sliding layer in landslides. *Canadian Geotechnical Journal* 40(1), 46-53.

Cai, F. and Ugai, K. 2011. A subgrade reaction solution for piles to stabilise landslides. *Géotechnique* 61(2), 143-151.

Chow, Y.K. 1996. Analysis of piles used for slope stabilization. *International Journal on Numerical and Analytical Methods in Geomechanics* 20(9), 635–646.

Chen, L.T. and Poulos, H.G. 1997. Piles subjected to lateral soil movements. *Journal Geotechnical and Geoenvironmental Eng.* 123(9), 802-811.

De Beer, E.E. and Carpentier, R. 1977. Discussion on the paper of Ito & Matsui (1975). *Soil and Foundations* 16(1), 68-82.

Di Laora, R,, Maiorano, R.M.S. and Aversa, S. 2017. Ultimate lateral load of slope-stabilising piles. *Géotechnique Letters* 7(3), 237-244.

Di Laora, R. and Fioravante, V. 2018. A method for designing the longitudinal spacing of slope-stabilising shafts. *Acta Geotechnica* 13(5), 1141-1153

Ellis, E.A., Durrani, I.K. and Reddish, D.J. 2010. Numerical modelling of discrete pile rows for slope stability and generic guidance for design. *Géotechnique* 60(3),185–195.

Fleming, K., Weltman, A., Randolph, M. and Elson, K. 2009. *Piling Engineering*. 3th ed. Taylor & Francis. London (UK and New York (NY).

Georgiadis, K., Sloan, S.W. and Lyamin, A.V. 2013. Undrained limiting lateral soil pressure on a row of piles. *Computers and Geotechnics* 54, 175-184.

Goh, A.T.C., Wong, K.S., The, C.I. and Wen, D. 2003 Pile response adjacent to braced excavation". *Journal Geotechnical and Geoenvironmental Eng.* 129(4), 383–386.

Guo, W.D. 2014. Elastic models for nonlinear response of rigid passive piles. *International Journal on Numerical and Analytical Methods in Geomechanics* 38(18), 1969–1989.

Hassiotis, S., Chameau, J.L. and Gunaratne, M. 1997. Design method for stabilization of slopes with piles. *Journal Geotechnical and Geoenvironmental Eng.* 123(4), 314–323.

Ito T, Matsui T (1975) Methods to estimate lateral force acting on stabilizing piles. *Soils and Foundations* 15(4): 43-59.

Ito, T., Matsui, T. and Hong, W.P. 1979. Design method for the stability analysis of the slope with landing pier. *Soils and Foundations* 19(4), 43-57.

Ito, T., Matsui, T. and Hong, W.P. 1981. Design method for stabilizing piles against landslide-one row of piles. *Soils and Foundations* 21(1), 21-37.

Ito, T., Matsui, T. and Hong W.P. 1982. Extended Design Method For Multi-Row Stabilizing Piles Against Landslide. *Soils and Foundations* 22(1), 1-13.

Jeong, S., Kim, B., Won, J. and Lee, J. 2003. Uncoupled analysis of stabilizing piles in weathered slopes. *Computers and Geotechnics* 30(8), 671–682.

Leung, C.F., Chow, Y.K., and Shen, R.F. 2000. Behaviour of pile subject to excavation-induced soil movement. *Journal Geotechnical and Geoenvironmental Eng.* 126(11), 947–954.

Kourkoulis, R., Gelagoti, F., Anastasopoulos, I. and Gazetas, G. 2011. Slope Stabilizing Piles and Pile-Groups: Parametric Study and Design Insights. *Journal Geotechnical and Geoenvironmental Eng ASCE* 137(7), 663–677.

Kourkoulis, R., Gelagoti, F., Anastasopoulos, I. and Gazetas, G. 2012. Hybrid method for analysis and design of slope stabilizing piles. *Journal Geotechnical and Geoenvironmental Eng ASCE* 138(1), 1–14.

Lei, G., Su, D. and Cabrera, M.A. 2022. Non-dimensional solutions for the stabilising piles in landslides in layered cohesive soils considering non-linear soil-pile interactions. *Géotechnique* 72(8), 737-751.

Poulos, H.G. 1995. Design of reinforcing piles to increase slope stability. *Canadian Geotechnical Journal*. 32(5), 808–818.

Poulos, H.G. 1996. A comparison of some methods for the design of piles through embankments. *Proc. XII Southeast Asian Geotechnical Conference*. Kuala Lumpur.

Viggiani, C. 1981. Ultimate Lateral Load on Piles used to Stabilize Landslides. *Proc. X ICSMFE*. Stockholm, Vol. 3, 555–560.

Viggiani, C., Mandolini, A. and Russo, G. 2012. *Piles and Pile Foundations*. Spon Press. London (UK) & New York (NY).

Wei, W.B. and Cheng, Y.M. 2009. Strength reduction analysis for slope reinforced with one row of piles. *Computers and Geotechnics* 36(7), 1176–1185.

Won, J., You. K., Jeong, S. and Kim, S. 2005. Coupled effects in stability analysis of pile–slope systems. *Computers and Geotechnics* 32(4), 304–315.

Yamin M and Liang RY (2010) Limiting equilibrium method for slope/drilled shaft system. *Int. J. Numer. Anal. Methods Geomech*. 34(10):1063–1075.